FRACTAL EARTHQUAKE SOURCE WITH SLIP PULSE GENERATES ACCELERATION TIME HISTORIES WITH FLAT SPECTRA

A. A. Gusev

Institute of Volcanology and Seismology, Petropavlovsk-Kamchatsky, Russia; e-mail: gusev@emsd.ru

The classical ω^{-2} model of earthquake source spectrum has strong empirical support; still, it has no consistent theoretical foundation. It is shown that one can explain ω^{-2} spectral behavior by involving a number of concepts regarding fault rupture: the fault asperity failure model of Das-Kostrov; the Andrews's concept, that the field of the stress drop over a fault is random fractal with amplitude spectrum of $1/k$ type; the running slip pulse rupture concept of Heaton; and the hypothesis, that the distance of propagation of Rayleigh waves excited by a failing spot on a fault is determined by the width of the slip pulse strip that in related with the propagating rupture. It is also assumed that over its width, this strip is filled by tortuous, multiply connected rupture front with the geometry of a random fractal line (polyline). To simulate seismic waves, a kinematic numerical model is designed that incorporates the described features. It generates realistic two-corner spectra; at high frequency, acceleration spectra are flat. The results enable one to explain properties of broad-band strong ground motion and to perform its practical simulation.

Keywords: earthquake source spectrum, fractal, stress drop, kinematic, accelerogram, self-similar.

INTRODUCTION. In 1967 г Aki [1] found, that the signal of displacement in body waves from an earthquake source has high-frequency spectral asymptotic of the ω^{-2} kind; then Hanks and McGuire [2] have found out that this assumption allows one to model ground accelerations in the epicentral zone. The mechanism generating commonly observed spectra of the ω^{-2} kind remains a puzzle: it is interesting to solve it, and the result may be interesting for applications.

THEORETICAL BASIS of MODEL. To study the problem at hand, a numerical model is constructed, based on the theory of asperity fault after Das and Kostrov [3, 4]. As a first step [3] they considered an infinite fault with zero friction, with a limited welded patch or "asperity", loaded with shear. During the failure of the asperity, the rupture front propagates that sweeps its surface; distribution of stress drop $\Delta\sigma(x, y)$ is thus created. In this process, surface waves are generated that run along surfaces of the fault, and also body waves P and S. Velocity $\dot{u}^{SH,\infty}(\xi, t)$ of SH wave in a far-field receiver at a point $\boldsymbol{\xi} = \{\xi_1, \xi_2, \xi_3\}$ is

$$\dot{u}^{SH,\infty}(\xi, t + R/c_S) = A\int_{\Sigma} \Delta\sigma(\mathbf{r}), \delta(t - \mathbf{r}\cdot\boldsymbol{\gamma}/c_S - t_{fr}(\mathbf{r}))dS; \quad A = \frac{\Re_{\mathcal{F}}^{SH}}{4\pi\rho\, c_S^2 r} \qquad (1)$$

where dot above indicates d/dt; $u^{SH,\infty}(\xi, t)$ is displacement signal, $\mathbf{r} = \{x, y, 0\}$ is a point of a source, $\mathbf{r}_h = \{x_h, y_h, 0\}$ is hypocenter; $R = |\,\boldsymbol{\xi} - \mathbf{r}_h|$, ρ is density, c_S is S-wave velocity, $\Re_{\mathcal{F}}^{SH}$ is the radiation pattern of SH waves for a *force* point source, Σ is the asperity patch, with characteristic size $2R_{ca} \ll R$, and element dS; $\delta(\cdot)$ is delta-function. The "∞"superscript symbolizes the case of infinite fault. Qualitatively, $u^{SH,\infty}(\xi, t)$ is a step ($H(t)$), smoothed by a window of duration $T_c \approx 2R_{ca}/v_r$, where v_r is the velocity of rupture front propagation, assumed to be close to c_S. T_c is close to the duration of rupture propagation. It is supposed that $\Delta\sigma(x, y) > 0$, therefore the signal (1) is a unipolar pulse. The area of this pulse (equal to final wave displacement $u^{SH,\infty}(\xi, \infty)$) is defined by integral "seismic force of a source"

$$F_0 = \int_\Sigma \Delta\sigma(\mathbf{r})dS \tag{2}$$

For the amplitude of velocity signal within its duration T_c, based on (1, 2) one can derive an estimate

$$\dot{u}^{SH,\infty}(\xi,t) \approx AF_0 / T_c \tag{3}$$

The model [3] has been developed further [4] for a fault with a frictionless region of finite size $2R_{ra}$. In this case Rayleigh waves do not run to infinity, but die away on the boundary of this region, where they are converted to body waves. Their contribution to far-field body wave creates an additional term to (1) with negative integral that accurately compensates the step-like behavior of $u^{SH,\infty}(\xi,t)$. In time, this term is lagged behind by the delay of, approximately, $T_{ra}=R_{ra}/c_R \approx R_{ra}/c_S$. As the result the displacement signal obtains the shape of unipolar pulse, common in seismology

$$u^{SH}(\xi,t) = A\int_\Sigma \Delta\sigma(\mathbf{r})G(t - r/c_S)dS \approx A(F_0/T_c)T_r \tag{4}$$

$$\text{with} \quad G(t) = H(t) - \int \Lambda(s)H(t-s)ds \tag{5}$$

where $G(t)$ is a signal from an elementary radiator. $\Lambda(\cdot)$ is a unit-area window function with characteristic time T_{ra}, thus $G(t)$ it is an asymmetric one-sided pulse, with instant leading edge and with gradual trailing edge; its duration is close to (1-2) T_{ra}. It is assumed further that $G(t)$ is the same for all **r**. . In numerical calculations, the particular $G(t)$ is set after [5]:

$$G(t) = H(t) - 0.5(1+\cos \pi t / T_{dec}); \quad t < T_{dec} \tag{6}$$

where T_{dec} =0.5T_{ra}; $G(t)$ =0 at $t> T_{dec}$. Therefore, the characteristic distance of decay of Rayleigh wave amplitude is assumed as $R_{dec} =c_R T_{dec}$.The body wave displacement pulse (4) with amplitude of the order AF_0T_{ra}/T_{ca} and duration of the order T_{ca} has the integral close to $AF_0T_{ra} = (A/c_S)\, F_0\, R_{ra} \approx (A/c_S)\, M_0$, where $M_0 \approx F_0R_{ra}$ is the seismic moment of the source [4,5]. Formulas similar to (1-4) hold also for *P* and *SV* waves.

In [4] the case is considered when Rayleigh waves propagate away (up to a distance R_{ra}) from a single asperity of the size $2R_{ca}$ « $2R_{ra}$. In [5,6,7], these results were applied to the multiple-asperity case. The case considered below is different (see Fig 1a). On one side, the propagation distance of Rayleigh waves, now denoted R_r, is thought to be much larger than fault spot size $dS^{0.5}$ that plays the role of "asperity" (R_r » $dS^{0.5}$). On another side, the earthquake source size $2R_c$ is assumed to be large as compared to R_r i.e., R_r « R_c, in difference with [5] . Shortly, $dS^{0.5}$« R_r «R_c

To permit Rayleigh waves to propagate, a spot of size $2R_r$ around a radiator dS located at a current point **r** of the rupture must be of low cohesion. Just this condition is realized when slip pulse [8] passes through the neighborhood of **r**, and one can believe that the slip-pulse width l of [8] is close to $2R_r$. In terms of rise time T_r, $2R_r \approx c_S\, T_r$; this assumption is critical for the present approach; further it is assumed that $R_r/R_c = C_H$.

As regards the $\Delta\sigma(x, y)$ function, it is assumed in [9], that it is self-similar stochastic random function with Fourier spectrum shape close to $1/k^{\beta}$ with $\beta\approx 1$; this hypothesis is generally supported by the results of inversions of the real sources, and is accepted in the following. The distribution law of $\Delta\sigma(x, y)$ is assumed lognormal, and the relative scatter of its values is defined through the coefficient of variation $CV_{\Delta\sigma} = (\mathrm{Var}(\Delta\sigma(x,y))^{0.5} / \mathrm{E}(\Delta\sigma(x,y))$. See Fig 1b for example.

In almost all models of earthquake sources the shape of the running rupture front is assumed to be a smooth line. However an expressed geometrical complexity of fronts is a necessary condition

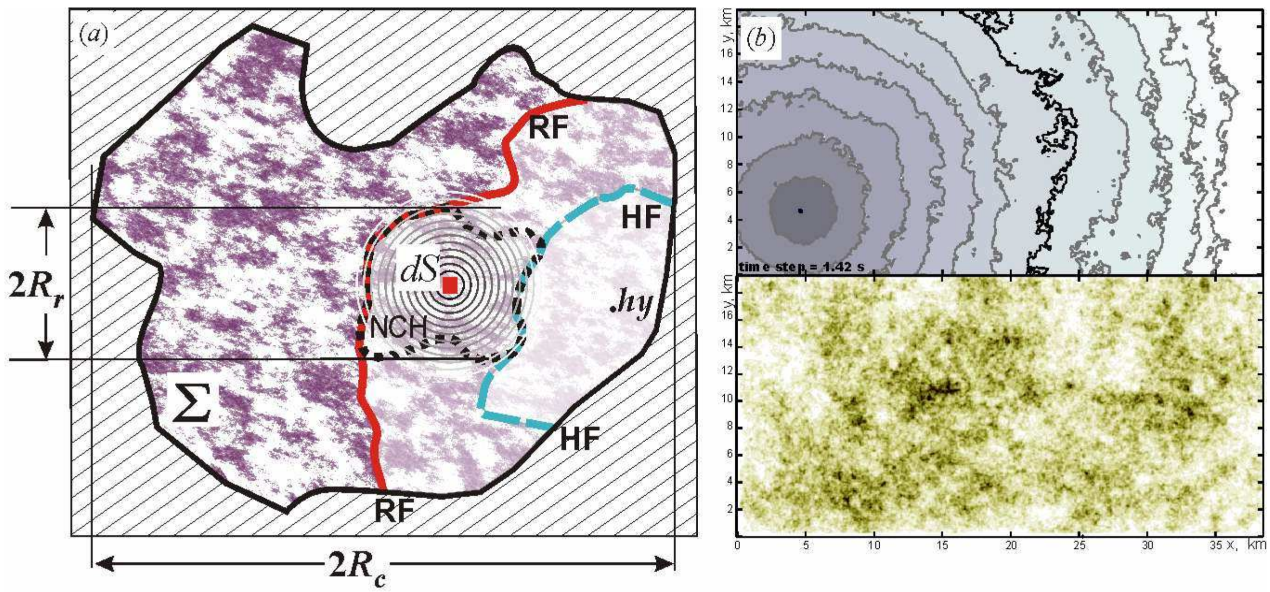

Fig. 1 (a) A cartoon depicting an earthquake source on an area Σ of the size $2R_c$. Indicated: ***hy*** - the hypocenter, RF - rupture front , HF - healing front. NCH (no cohesion) is a patch on the fault, of the size $2R_r$ (dotted contour) where the propagation of Rayleigh waves radiated from dS is confined (the particular plotted patch corresponds to particular dS only!). Rupture front and healing front are not strictly defined entities, they are understood as boundaries of a strip where the actual, wiggling and fragmented, fractal front is localized. (b) - example random fields $t_{fr}(x, y)$ and $\Delta\sigma(x, y)$ on a specimen of the simulated source. Wiggling isolines depict positions of the fractal front each 1.4 s. Shades of gray code time: the later, the lighter. The bold line gives a particular example position of the front. Below an isotropic random field $\Delta\sigma(x, y)$ with a spectrum $\propto 1/k$ is depicted; shade intensity reflects amplitude; maxima are darker.

for formation of usually observed incoherence of high-frequency radiation from a source. As in [10], it is assumed that the rupture front has fractal geometry and is a "lacy" polyline (with "islands" and "lakes") that fills a strip of the width $2R_r$. To form such a shape, the moment of failure $t_{fr}(\cdot)$ at a point $\mathbf{r} = \{x, y\}$ is defined by the sum of two terms:

$$t_{fr}(x, y) = R(x, y) + S(x, y) \qquad (6)$$

Here $R(x, y)$ is a stochastic function; it provides fragmented shape of the front at big k. In simulation, $R(x, y)$ is a sample self-similar function, with spectrum $\propto 1/k^{\delta}$ and with the uniform distribution law in the interval $[0\ 2T_r]$. The $S(x, y)$ term provides regular behavior of rupture, best seen at small k, it is taken as $S(x, y) = |\mathbf{r} - \mathbf{r}_h|/v_r$; $\mathbf{r}_h$ is the hypocenter (providing the top of the cone $t = S(x, y)$). For more realistic appearance, slight long-wavelength perturbation is added to $S(x,y)$.

SIMULATION AND ITS RESULTS. The procedure of numerical calculation was coded as described above; it includes (the accepted values in parentheses): (a) the choice of: the size of a rectangular source (38×19 km), time step dt (0.025 s) , distance step dx (0.075 km); v_r (3.0 km/s); c_S (3.5 km/s); the hypocenter position $\mathbf{r}_h$; (b) the setting of parameters: β (1.0), C_H (0.06), $CV_{\Delta\sigma}$ (0.8), δ (1.4); (c) generation of sample random fields $t_{fr}(x, y)$ and $\Delta\sigma(x, y)$; (d) calculation of $\dot{u}^{SH,\infty}(\xi, t)$ according to Equation 1 for a ray along normal to the fault (the present analysis is confined by this case); (e) calculation of $u^{SH}(\xi, t) \equiv u(t)$ based on Equation 4; (f) determination of normalized displacement spectrum $u_n(f)$ calculated from $u(t)$) as the amplitude of Fourier transform, smoothed at high frequencies, and normalized by division by M_0 ; and also of the associated acceleration spectrum $\ddot{u}_n(f)$. See typical results on Fig. 2.

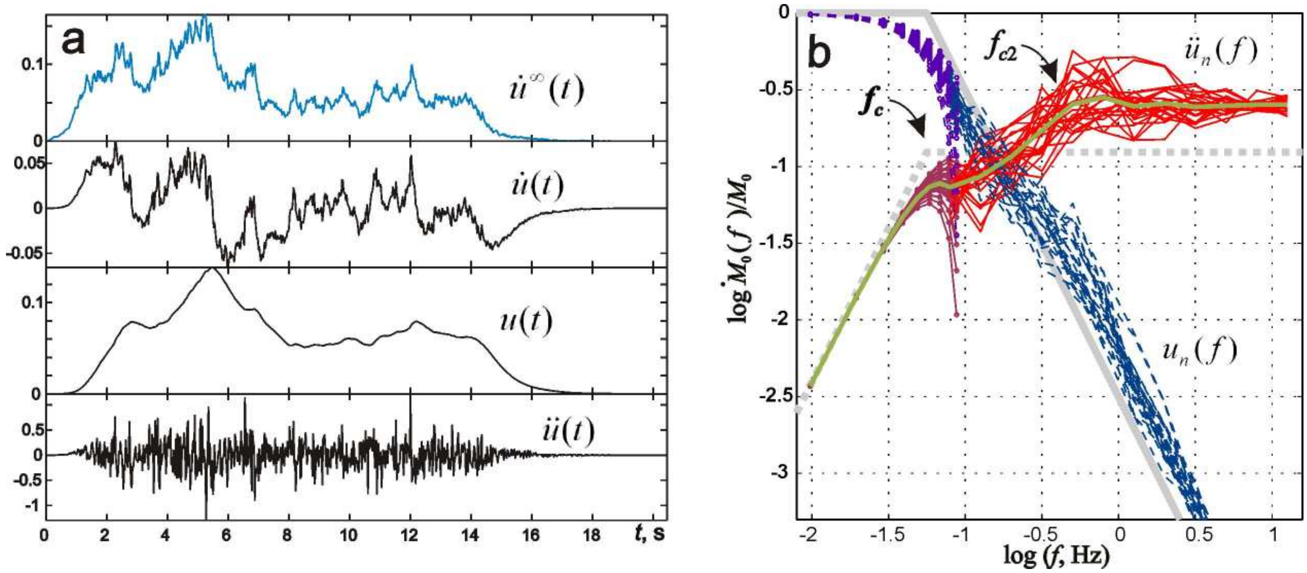

Fig. 2. Typical results of simulation. (a) - signals $\dot{u}^{\infty}(t)$, $\dot{u}(t), u(t)$ и $\ddot{u}(t)$ at the receiver. (b) - spectra $u_n(f)$ и $\ddot{u}_n(f)$, raw (on the left) and smoothed (on the right): 25 individual spectra (red) and their average (yellow). Gray lines - idealized spectra for the single-corner ω^{-2} model. The main corner-frequency f_c is set as $1/2\pi T_{rms}$, where T_{rms}^2 is the second normalized central power moment for $u(t)$.

DISCUSSION AND CONCLUSION. Looking at Fig 2a one can perceive that signals $\dot{u}(t), u(t)$ и $\ddot{u}(t)$ qualitatively agree with observed records of real earthquakes. On Fig. 2b one can see that the smoothed acceleration spectrum is flat, according to ω^{-2} model. Also, the well-expressed second corner-frequency f_{c2} is present (it however disappears at C_H of around 0.1 and above). Both these features agree well with observations. The C_H parameter controls the spectral shape to a large degree. At a given (M_0 , L) combination, when the width l of the slip pulse is getting more narrow, acceleration spectral level increases, and f_{c2} increases as well. One can conclude in general that:

(1) An internally consistent and theoretically well founded broad-band kinematic model of earthquake source is devised and realized numerically. It reproduces two most prominent features of HF source spectra: ω^{-2} spectral shape and second corner frequency

(2) The developed simulation technique has a potential for simplified simulation of strong ground motion. To its advantage, this technique is capable to predict consistently the variability of radiation properties that occurs at a given (M_0, L) combination.

REFERENCES

[1] K. Aki. 1967, J. Geophys. Res. 72, 1217–1231.
[2] T.C. Hanks, and R.K. McGuire. 1981, Bull. Seismol. Soc. Amer. 71, 2071–2095.
[3] S. Das and B.V. Kostrov. 1983, J. Geophys. Res. 88, 4277-4288.
[4] S. Das and B.V. Kostrov. 1986. In: Earthquake source mechanics, 91-96, Washington, Amer. Geophys. Union.
[5] J. Boatwright. 1988, Bull. Seismol. Soc. Amer., 78, 489-508.
[6] A.A. Gusev. 1988, Volcanology and Seismology, #1, 41-55 (in Russian).
[7] A.A. Gusev. 1989, Pure Appl. Geophys., 130, 635-660.
[8] T.Heaton. 1990, Phys. Earth Planet. Inter., 64, 1–20
[9] D.J. Andrews. 1980, J. Geophys. Res., 78, 3867–3877.
[10] A.A. Gusev. 2012, Pure Appl. Geophys. 168, 155-200.